

EXHIBIT N

Udan et al., *Nat Cell Biol* 5: 914-920 (2003)

Hippo promotes proliferation arrest and apoptosis in the Salvador/Warts pathway

Ryan S. Udan^{1,2,4}, Madhuri Kango-Singh^{2,4}, Riitta Nolo², Chunyao Tao² and Georg Halder^{1-3,5}

Proliferation and apoptosis must be precisely regulated to form organs with appropriate cell numbers and to avoid tumour growth^{1,2}. Here we show that Hippo (Hpo), the *Drosophila* homologue of the mammalian Ste20-like kinases³, MST1/2, promotes proper termination of cell proliferation and stimulates apoptosis during development. *hpo* mutant tissues are larger than normal because mutant cells continue to proliferate beyond normal tissue size and are resistant to apoptotic stimuli that usually eliminate extra cells. Hpo negatively regulates expression of Cyclin E to restrict cell proliferation, downregulates the *Drosophila* inhibitor of apoptosis protein DIAP1, and induces the proapoptotic gene *head involution defective* (*hid*) to promote apoptosis. The mutant phenotypes of *hpo* are similar to those of *warts* (*wts*), which encodes a serine/threonine kinase of the myotonic dystrophy protein kinase family^{4,5}, and *salvador* (*sav*), which encodes a WW domain protein that binds to Wts^{6,7}. We find that Sav binds to a regulatory domain of Hpo that is essential for its function, indicating that Hpo acts together with Sav and Wts in a signalling module that coordinately regulates cell proliferation and apoptosis.

To identify genes that regulate tissue growth, we performed a mutagenesis screen by using the *eyFLP* system⁸ and isolated three complementation groups that showed similar overgrowth phenotypes. These were *sav* (also known as *shar-pei*)^{6,7}, *wts*^{4,5} and a previously uncharacterized locus that we named 'hippo' (*hpo*) because of the dark, folded and overgrown cuticle of the mutant heads (Fig. 1, and see Supplementary Information, Fig. S1).

We isolated four alleles of *hpo* (*hpo*^{KC202}, *hpo*^{KC203}, *hpo*^{KC221} and *hpo*^{KS240}) that all showed similar overgrowth phenotypes. Adult mutant heads were enlarged, with larger eyes and expanded and folded cuticle on head and antennae (Fig. 1a, b). *hpo*^{KC202} mutant cells showed overgrowths on head cuticle (Fig. 1a, b), halteres (Fig. 1c, d), thorax, wings and legs (data not shown). Notably, the positions of pattern elements such as ommatidia, bristles and ocelli were relatively normal (Fig. 1a, b), and overgrown structures differentiated proper cell types (Fig. 1a–e). We therefore conclude that Hpo is a general

growth regulator required to restrict cell number and tissue size in adult structures.

Analysis of *hpo*^{KC202} mutant clones in adult eyes by thin sections showed that there was a considerable increase in spacing between photoreceptor clusters in mutant regions as compared with wild-type regions (Fig. 1e, double arrow). This was due to a large increase in numbers of interommatidial cells, which were evident in *hpo*^{KC202} mutant mid-pupal retinæ (Fig. 1f, g). These extra cells eventually differentiated into extra bristles and pigment cells. In contrast to the interommatidial cells, most *hpo*^{KC202} mutant ommatidia had normal numbers of photoreceptor (Fig. 1e), cone and primary pigment cells (Fig. 1e–g). Notably, the sizes of all cell types were normal in mutant eyes, although the morphology of photoreceptors was often abnormal (Fig. 1e). We also analysed the expression of *Elav*, a marker for differentiating photoreceptor cells, and the R8 marker *Senseless* (*Sens*) to test whether *hpo* affects pattern formation during development. The initial spacing of R8 cells and the number of photoreceptor cells per ommatidium were normal in *hpo*^{KC202} mutant clones (Fig. 1h, i). Thus, mutations in *hpo* primarily affect tissue size but not patterning or differentiation.

We tested the effects of loss of Hpo function on cell proliferation by analysing the pattern of bromodeoxyuridine (BrdU) incorporation, which marks cells in S phase (Fig. 1j, k). In wild-type eye discs, BrdU-incorporating cells were randomly distributed anterior to the morphogenetic furrow, arrested in G1 in the furrow, and started either to differentiate into photoreceptor cells or to undergo an additional round of cell division referred to as the second mitotic wave posterior to the furrow (Fig. 1j, arrowhead). After the second mitotic wave, cells cease proliferation and differentiate into the remaining photoreceptor, cone, pigment and bristle cells⁹.

Mutant cells in eye discs that were almost completely mutant for *hpo*^{KC202} (subsequently referred to as *eyFLP hpo*^{KC202} eye discs because the clones were induced by *eyFLP*) properly synchronized their cell cycles in the furrow (Fig. 1k, arrow) and progressed through the second mitotic wave (Fig. 1k, arrowhead). In contrast to wild-type, however, cells in *eyFLP hpo*^{KC202} eye discs showed ectopic incorporation of BrdU after the second mitotic wave (Fig. 1k, asterisk). DNA synthesis was followed by cell division, as assessed by the ectopic expression of phospho-

¹Program in Developmental Biology, Baylor College of Medicine, Houston, Texas 77030, USA. ²Department of Biochemistry and Molecular Biology, M. D. Anderson Cancer Center, Houston, Texas 77030, USA. ³The Genes and Development Graduate Program, The University of Texas Graduate School of Biomedical Sciences, M. D. Anderson Cancer Center, Houston, Texas 77030, USA. ⁴These authors contributed equally to this work. ⁵Correspondence should be addressed to G.H. (e-mail: ghalder@mdanderson.org).

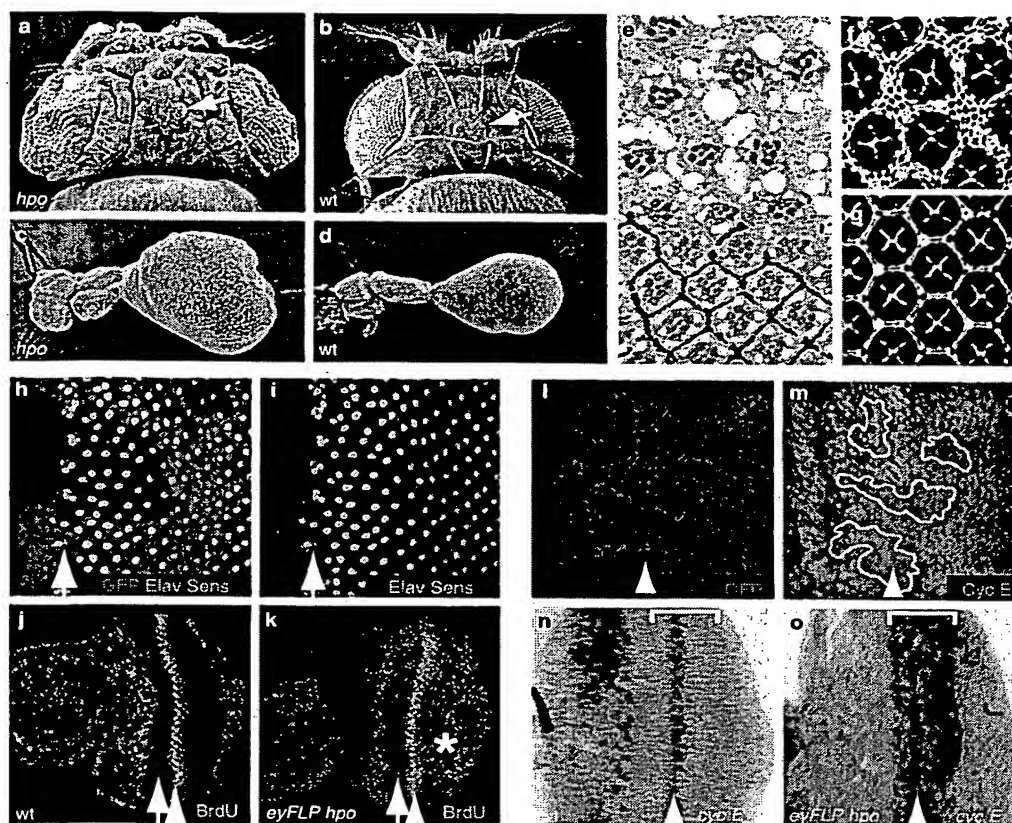


Figure 1 *hippo* regulates tissue size, cell-cycle arrest and expression of Cyclin E. (a, b) Dorsal view SEM images of a fly with a *hpo*^{KC202} mutant head (a) produced by *eyFLP*-induced mitotic recombination⁸ and a wild-type fly (b). The mutant tissue is severely overgrown and folded. Ocelli (arrows), bristles and hairs differentiated normally. (c) Haltere with *hpo*^{KC202} mutant clones. (d) Wild-type haltere. The mutant haltere was generated by heat-shock-induced Flippase expression. (e) Plastic thin section through an adult eye that is mosaic for *hpo*^{KC202} mutant cells. Mutant tissues are visualized by the absence of pigment granules in pigment and photoreceptor cells. Spaces between photoreceptor clusters are larger in mutant than in wild-type tissues (double arrow), but photoreceptor numbers are normal in mutant ommatidia. (f, g) Mid-pupal retinæ stained with anti-Dlg antibodies to visualize cell outlines. (f) *hpo*^{KC202} mutant mid-pupal retina shows excess interommatidial cells as compared with wild type (g). (h, i) *hpo*^{KC202} mutant clones, marked by the absence of green fluorescent protein (GFP; red in h),

in a third instar eye disc stained for Sens (green) and Elav (blue) expression, which is shown separately in i. Mutant clones show normal patterning. (j) Wild-type eye imaginal discs stained for BrdU incorporation (green). Cells arrest in G1 in the morphogenetic furrow (arrow) and non-differentiating cells go through one synchronous S phase in the second mitotic wave (arrowhead). (k) An *eyFLP hpo*^{KC202} mosaic eye disc shows ectopic cell proliferation posterior to the second mitotic wave (asterisk). (l, m) *hpo*^{KC202} mutant cells, marked by the absence of GFP (red in l), have increased Cyclin E protein (green in m) in and around the second mitotic wave (arrowhead). (n, o) Cyclin E mRNA expression in wild-type and in an *eyFLP hpo*^{KC202} mosaic eye disc. Cyclin E mRNA is upregulated in a band straddling the second mitotic wave in *eyFLP hpo*^{KC202} eye discs (white brackets). White lines mark clone boundaries. Arrows indicate the morphogenetic furrow (h–k). Arrowheads indicate the second mitotic wave (j–o). Anterior is to the left for all discs.

rylated histone H3 (PH3), which marks mitotic chromosomes (data not shown). Thus, Hpo mutant cells fail to arrest in G1 and continue to proliferate. This phenotype is cell autonomous and ectopic proliferation is restricted to uncommitted precursor cells and not observed in differentiating photoreceptor cells (see Supplementary Information, Fig. S2). Furthermore, Cyclin E, which is limiting for S-phase initiation in imaginal disc cells¹⁰, was cell autonomously upregulated in *hpo*^{KC202} mutant clones (Fig. 1l, m). Likewise, Cyclin E messenger RNA was upregulated in and around the second mitotic wave in *eyFLP hpo*^{KC202} eye discs (Fig. 1n, o). Thus, the transcriptional repression of Cyclin E expression is probably an important downstream effect of Hpo to promote proliferation arrest of uncommitted precursor cells.

Because extra interommatidial cells are normally removed by developmentally induced apoptosis, the phenotype of *hpo*^{KC202}

mutant retinæ indicated that Hpo was required for apoptosis in addition to cell proliferation arrest. Indeed, in contrast to wild-type, clones of *hpo*^{KC202} mutant cells lacked apoptotic cells (Fig. 2a, b), showing that *hpo* is required for developmentally regulated apoptosis in the retina. We next tested whether *hpo* mutant cells were protected from ectopically induced cell death. Overexpression of Hid in the developing eye induces apoptosis and results in loss of eye structures¹¹ (Fig. 2c). *hpo*^{KC202} loss-of-function partially rescued cell death in eye discs that ectopically expressed Hid (Fig. 2d–f).

The proapoptotic genes *hid*, *reaper*¹², *grim*¹³, *sickle* (*skl*)^{14–16} and *Jafra2* (ref. 17) induce apoptosis by activating caspase cascades through direct targeting of DIAP1 for auto-ubiquitination and degradation, which in turn liberates caspases from DIAP1-mediated inhibition^{15,18–21}. *hpo*^{KC202} mutant clones showed an increase in DIAP1

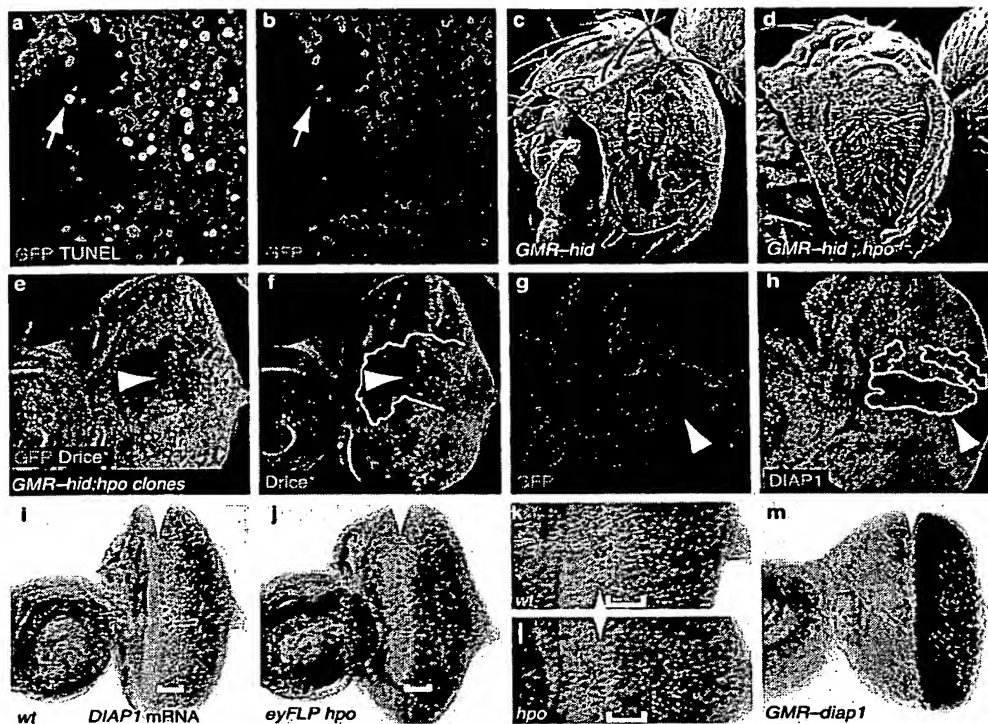


Figure 2 *hpo* is required for apoptosis in eye development and regulates DIAP1. (a, b) Confocal image showing TUNEL labelling (green, arrow) of a pupal retina mosaic 30 h after pupariation for *hpo*^{KC202} mutant clones. Mutant cells are marked by the absence of GFP expression (red). (c) SEM image of a *GMR-hid* transgenic fly head. (d) Adult head of a *GMR-hid* fly mosaic for *hpo*^{KC202} mutant clones. (e, f) *hpo*^{KC202} mutant clones (GFP negative) in an eye disc expressing *GMR-hid*, labelled to detect expression of activated Drice* (Drice*, green), which is shown separately in f. Arrowhead points to a mutant region with downregulated Drice* expression.

(g, h) *hpo*^{KC202} mutant clones (GFP-negative) upregulate DIAP1 expression (green), which is shown separately in h. (i, j) DIAP1 mRNA expression in wild-type and *eyFLP hpo*^{KC202} eye discs. DIAP1 mRNA is upregulated posterior to the morphogenetic furrow in *eyFLP hpo*^{KC202} discs. (k, l) Higher magnifications of images in i and j, respectively. (m) Overexpression of DIAP1 mRNA in *GMR-diap1* eye discs for comparison. White arrowheads mark the morphogenetic furrow in i–m, and white brackets mark the region of upregulation of DIAP1 mRNA in i–m. White lines mark clone boundaries in f and h. Anterior is to the left for all discs.

protein (Fig. 2g, h) and mRNA (Fig. 2i–l). Regulation of DIAP1 might include transcriptional mechanisms because DIAP1 mRNA was upregulated just behind the furrow (Fig. 2i–l). The increase in DIAP1 might protect cells from apoptosis induced both in normal development and by ectopic expression of Hid. Notably, *sav* and *wt* mutants showed similar defects in proliferation arrest and apoptosis^{6,7} (data not shown).

To identify the *hpo* gene, we mapped the lethality associated with the mutation through meiotic mapping by using P-elements and single nucleotide polymorphisms (SNPs) as markers^{6,22}, and found different mutations in CG11228 in all four *hpo* alleles (see Supplementary Information, Fig. S3). Transgenes containing the whole genomic region of CG11228 between the proximal and distal neighbouring genes rescued the lethality of *hpo* trans-heterozygotes (data not shown), showing that CG11228 indeed encodes Hpo. *hpo* was ubiquitously expressed during imaginal disc development, consistent with its requirement for proper proliferation arrest in these tissues (see Supplementary Information, Fig. S3).

Hpo is an orthologue of the mammalian Ste20-family kinases MST1 and MST2 (MST1/2)³. MST1/2 are implicated in the activation of mitogen-activated protein kinase (MAPK) cascades and in regulating apoptosis^{3,23–25}. Hpo contains three highly conserved domains: an

amino-terminal kinase domain; a central autoregulatory domain that inhibits kinase activity; and a domain implicated in dimerization²⁶ and binding to Sav (see below) at its very carboxy terminus. Notably, the protein produced from all four *hpo* alleles is truncated after the kinase domain, and the highly conserved dimerization domain that mediates complex formation with Sav is deleted (see Supplementary Information, Fig. S4). All four alleles contain recessive loss-of-function mutations and are homozygous lethal at the first-second larval instar stage.

Two independent clones of *hpo* were isolated in a yeast two-hybrid screen by using Sav as bait. Both clones contained the autoregulatory and dimerization domains (Fig. 3a). To characterize this interaction further, we produced ³⁵S-labelled Hpo and Sav proteins by coupled *in vitro* transcription and translation, and assayed them for complex formation by co-immunoprecipitation. Full-length Sav co-purified Hpo, and systematic deletion analyses showed that the dimerization domain of Hpo and the conserved Sav-specific domain (SD) of Sav were both necessary and sufficient for this interaction (Fig. 3b; see also Supplementary Information, Fig. S5). The dimerization domain of Hpo was also necessary and sufficient for dimerization of Hpo itself, similar to its vertebrate homologue MST1. However, Sav and Hpo did not form tetrameric complexes in our assay.

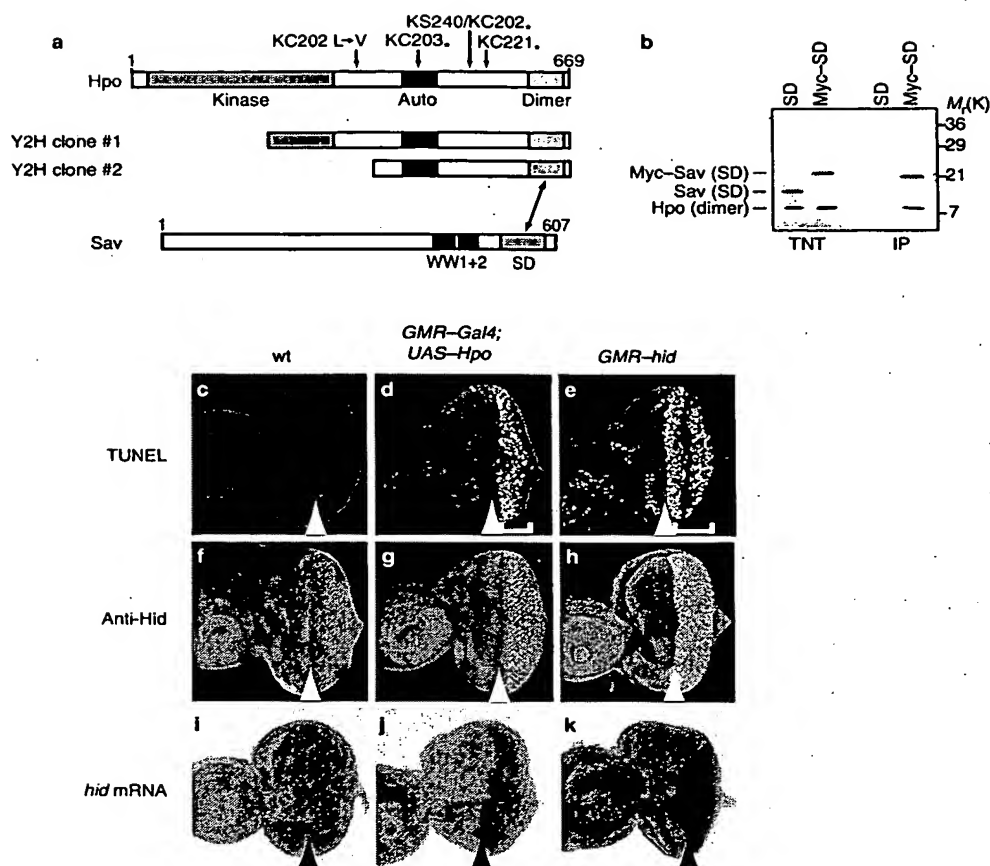


Figure 3 Hpo is a Ste20 family kinase that interacts with Sav and induces apoptosis. (a) Full-length Hpo protein with its three conserved domains and the positions of mutations in *hpo* alleles. Two cDNA clones identified in the yeast two-hybrid (Y2H) screen using Sav as a bait are shown below the full-length protein. Both clones contain the dimerization and autoregulatory domains. Sav contains three conserved domains: a doublet of WW domains, and an 'SD domain' of 69 amino acids that is specific to Sav and its orthologues. (b) Immunoprecipitation of the Sav-specific domain (Myc-SD) co-purified the dimerization domain of Hpo.

Thus, the SD domain complexes with the dimerization domain of Hpo (double arrow in a). S^{35} -labelled SD, SD-Myc and Hpo dimer domains were produced by *in vitro* transcription and translation (TNT) and analysed, together with the immunoprecipitates, by SDS-PAGE and autoradiography. (c-k) Overexpression of Hippo induces apoptosis. Wild-type, *GMR-Gal4; UAS-hpo* and *GMR-hid* eye discs were analysed for DNA fragmentation by TUNEL labelling (c-e), and for expression of Hid protein (f-h) and mRNA (i-k) by *in situ* hybridization. Arrowheads mark the morphogenetic furrow.

The interaction between Hpo and Sav is probably direct because it was also observed in yeast, which lacks this signalling pathway. All four *hpo* alleles produce C-terminally truncated proteins in which the region that interacts with Sav is deleted, indicating that the interaction between Hpo and Sav is important *in vivo*. The previously identified *sav^{shrp6}* allele specifically deletes the SD domain and causes phenotypes that are as strong as those of *sav* null alleles, further supporting this conclusion. The other conserved domains of Sav, the two WW domains, bind to Wts⁷. Thus, Sav may act as a scaffold to assemble signalling complexes comprising Hpo and Wts kinases.

Overexpression of several kinases including members of the Ste20 family has been used successfully in yeast, cell culture and *Drosophila* to activate signalling pathways³. Thus, overexpression of human MST1/2 in cell culture activates caspases and triggers apoptosis²⁴. Ectopic expression of wild-type Hpo during imaginal disc development resulted in loss of eye, head and wing tissues through the arrest of cell proliferation and the induction of apoptosis (Fig. 3,4). By contrast,

overexpression of a kinase-dead variant of Hpo, Hpo^{K71R}, did not result in smaller structures, but partially rescued the phenotypes caused by overexpressing wild-type Hpo (Fig. 4c,d; see also Supplementary Information, Fig. S6). Overexpression of Hpo^{Δauto}, a hyperactive form of Hpo, produced phenotypes similar to those caused by overexpressing wild-type Hpo (data not shown). The Hpo^{Δauto} construct carries a deletion that is analogous to a deletion in human MST1 that causes an increase in kinase activity *in vitro*²⁶. Thus, kinase activity is required for Hpo action and Hpo^{K71R} is acting as a dominant-negative form of Hpo, suggesting that overexpression of Hpo activates its pathway.

GMR-driven Hpo overexpression in the eye disc caused large amounts of apoptosis, similar to *GMR*-driven Hid expression (Fig. 3c-e). Hpo and Hid expression induced DNA fragmentation, activated Drice caspase, downregulated DIAP1 and induced nuclear condensation, which are all hallmarks of apoptosis (Fig. 3c-e; see also Supplementary Information, Fig. S6d-l). The small head and wing

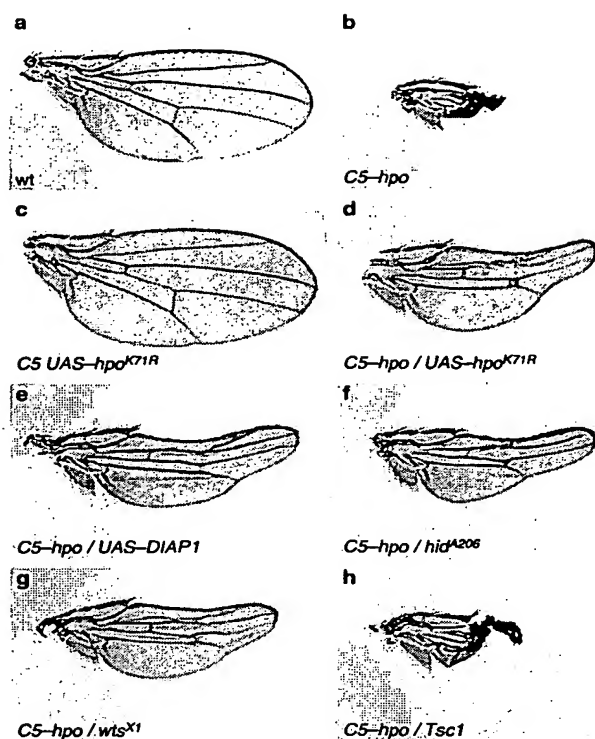


Figure 4 Hid and Wts are required for Hippo action. Cell death induced by Hpo overexpression is rescued by coexpressing kinase-dead Hpo or DIAP1 or by reducing the copy number of *hid* or *wts*. (a–c) Wings of adult flies that were wild type (a), overexpressing UAS-Hpo (b) and overexpressing UAS-Hpo^{K71R}, a kinase-dead mutant of Hpo (c), in the developing wing pouch using the *C5-Gal4* driver. (d–g) The *C5-Gal4*-driven UAS-Hpo phenotype is partially rescued by coexpressing Hpo^{K71R} (d), coexpressing DIAP1 (e), heterozygosity for *hid*^{A206} (f) or heterozygosity for *wts*^{X1} (g). (h) The *C5-GAL4* driven UAS-Hpo phenotype is not affected by the reduction of one copy of *Tsc1*.

phenotypes were partially suppressed by coexpression of DIAP1 and of p35, a general caspase inhibitor (Fig. 4e and data not shown). We also analysed expression of the proapoptotic gene *hid* that is required for developmentally regulated apoptosis observed during wild-type eye development²⁷.

GMR-driven Hpo expression upregulated *hid* mRNA and protein (Fig. 3f–k) but did not effect *grim* or *reaper* mRNA (data not shown). The small wing and eye phenotypes caused by Hpo overexpression were partially rescued by heterozygosity for *hid*, indicating that Hid is crucial for Hpo to exert its effects (Fig. 4f). Similarly, heterozygosity for *wts* suppressed the ectopic Hpo phenotype, suggesting that Hpo requires *wts* for its action (Fig. 4g). However, heterozygosity for *Tsc1*, a gene that functions in the target of rapamycin (TOR) signalling pathway that regulates cell growth, did not affect the Hpo overexpression phenotype (Fig. 4h).

Hpo thus seems to regulate apoptosis at several levels. On the one hand, Hpo negatively regulates DIAP1 to promote apoptosis. The increase in DIAP1 in *hpo* mutant clones protect cells from Hid-induced apoptosis, indicating that Hpo effects cell death downstream of Hid. On the other hand, Hpo seems to act upstream of Hid, because overexpression of Hpo upregulates Hid expression and causes Hid-dependent

cell death. In naturally occurring cell death pathways that require Hpo activity, such as the killing of interommatidial cells, a death-inducing signal may activate Hpo, which in turn may induce expression and activation of Hid, as well as downregulation of DIAP1 to trigger apoptosis.

It has been shown that the activity of Hid is regulated at the transcriptional and posttranslational level and that *hid* is required for apoptosis in the retina^{27,28}. MAPK, for example, promotes cell survival by downregulating Hid activity through direct phosphorylation and through transcriptional mechanisms that depend on the downstream transcription factor Pointed^{27–29}. Although we have not detected significant changes of MAPK phosphorylation either in Hpo mutant clones or by Hpo overexpression (data not shown), subtle effects of Hpo on MAPK activity may contribute to the effect of Hpo on Hid activity and apoptosis. Determining whether *hid* induction by Hpo is a direct effect or a secondary consequence of Hpo-induced cell death, however, requires further investigation. Because Hpo is expressed ubiquitously, its activity is probably regulated by posttranscriptional mechanisms such as phosphorylation. Indeed, the activities of the mammalian homologues of Hpo, MST1/2, are regulated by phosphorylation during stress-induced cell death³⁰.

The Hpo/Sav/Wts signalling pathway is unique in that it regulates apoptosis and proliferation. In fact, the *hpo* mutant overgrowth phenotypes are the outcome of deregulated cell proliferation, which generates extra cells, along with a lack of apoptosis, which allows extra cells to survive and to contribute to adult structures. Hpo, Wts and Sav mutants specifically affect cell numbers but not cell size, in contrast to other growth regulators such as InR signalling, Ras and Myc, which typically affect both cell size and cell number^{31,32}. In addition, the function of Hpo/Sav/Wts signalling is distinct from mechanisms directing cell-cycle exit during terminal differentiation because Hpo, Wts and Sav are required for cell proliferation arrest of uncommitted precursor cells but not differentiating cells⁶ (Fig. 1). Because of this specificity for precursor cells, only the last cell types to differentiate in the retina, namely the interommatidial pigment and bristle cells, are produced in excess, whereas the number of photoreceptor and cone cells is normal in mutant ommatidia.

Wts negatively regulates the activity of Cdc2/Cyclin A³³, and Sav, Wts and Hpo negatively regulate Cyclin E^{6,7}. Thus, excessive activity of Cdc2/Cyclin A and Cyclin E may contribute to drive cell proliferation of mutant cells. The promotion of cell-cycle progression alone, however, cannot account for the excess growth (mass accumulation) of mutant tissues¹⁰. Thus, Hpo/Sav/Wts signalling must regulate additional targets to restrict cell growth and cell proliferation. Hpo, Wts and Sav are highly conserved in vertebrates. As in *Drosophila*, the mammalian homologues of Hpo, MST1/2, have been implicated in regulating apoptosis. LATS1 acts as a tumour suppressor gene in vertebrates³³ and the human orthologue of Sav (hWW45) is mutated in cancer cell lines⁷. It will be interesting to determine whether MST1/2 signalling is downregulated in cancer cells. □

METHODS

Fly stocks. We isolated *hpo* and *wts* mutants in *eyFLP*-mediated ethylmethane sulphonate (EMS) mutagenesis screens on the 2R and 3R chromosome arms. Four alleles were recovered for both *hpo* (*hpo*^{KC202}, *hpo*^{KC203}, *hpo*^{KC221} and *hpo*^{KS240}) and *wts* (*wts*^{FA78}, *wts*^{GK40}, *wts*^{GX24} and *wts*^{HH38}). These *wts* alleles may be hypomorphic, because eye discs mutant for a *wts* null allele (*wts*^{X1}) have a stronger phenotype^{4,5}. Flies with heads that were almost completely homozygous mutant for *hpo*, *wts* and *sav* had the following genotypes: *y w eyFLP; FRT82B/FRT82B cl p[w⁺]* (control clones); and *y w eyFLP; FRT 42D hpo*^{KC202}/*FRT 42D cl p[w⁺]*, *y w eyFLP; FRT82B wts*^{FA78}/*FRT82B cl p[w⁺]* and *y w eyFLP; FRT82B sav*^{hhp1}/*FRT82B cl p[w⁺]* (where *cl* stands for a cell lethal mutation). The phenotypes of *hpo*^{KC203} and *hpo*^{KC221} mutant heads were

weaker (data not shown). Other stocks used were *C5-GAL4*, *ey-GAL4*, *GMR-GAL4*, *UAS-p35*, *GMR-hid*, *th hid^{A206} ri/TM6B*, *Tsc1^{IQ69}* and *UAS-DIAP1*.

Mapping of *hippo*. Meiotic mapping of *hippo* with P-elements was done essentially as described^{6,22}. Flies carrying *hpo^{KC202}*, *hpo^{KC203}* or *hpo^{KS240}* were crossed to flies carrying one of the five P-elements: *y w*; *P[GT1]BG2803*, *y w*; *P[GT1]BG2222*, *y w*; *P[lacW] l(2)k10809/CyO*, *y w* *P[EP]mei-W68^{EP1144}* and *y w* *P[EP]EP628* (<http://flypush.imgen.bcm.tmc.edu/pscreen>). Trans-heterozygous virgin females (*y w/y w*; *hpo/P[w⁺]*) were crossed to males of the genotype (*y w/Y*; *hpo/P[w⁺]*). Recombinant flies that were white (+/*hpo*) were counted, and recombination frequencies determined. We analysed three SNPs in recombinants between *hpo* (FRT chromosome) and *P[EP]EP628* to map recombination breakpoints: SNP107 (ref. 22), SNP H1 and SNP H2, which were found by sequencing 1-kb fragments amplified by polymerase chain reaction (PCR) in the *smooth (sm)* gene (~14,365 kb), and the genomic region between CG15904 and *sm* respectively.

Generation of transgenic flies. *Hpo* wild-type and mutant open reading frames (ORFs) were amplified by PCR by using complementary DNA clone RE21564 as a template, cloned into the *EcoRI*-*XbaI* sites of the pUAST vector³⁴ and used to generate transgenic flies. *UAS-hpo* contains the full ORF (amino acids 1–669), whereas *UAS-hpo[Δauto]* (amino acids 1–354 and 466–669) and the kinase-dead mutant, *UAS-hpo[K71R]*, contain mutant ORFs. We established and tested six or more independent lines for each construct. The genomic rescue construct was generated by PCR amplification of a 4,371-bp fragment from wild-type genomic DNA encompassing the whole region of CG11228 and overlapping 100 bp on either side into the neighbouring ORFs. This PCR-amplified fragment was cloned in the *EcoRI* site of pCaSpeR4 and transformed into flies by standard procedures. Six out of six transgenic lines rescued the lethality of *hpo* trans-heterozygotes.

Electron microscopy, immunohistochemistry and cell death assays. Scanning electron microscopy (SEM) of adult flies was done by the HMDS method⁶. We stained imaginal discs as described⁶ with the following antibodies (dilutions): rat anti-Elav (1:30), rabbit anti-Dlg (1:2,000; a gift from K. Choi), rabbit anti-Drice (1:2,000; from B. Hay), guinea-pig anti-Dlg (1:2,000; from P. Bryant), guinea-pig anti-Sens (1:1,000; from H. Bellen), mouse anti-BrdU (1:50; from Becton Dickinson, San Jose, CA), mouse anti-DIAP1 (1:200; from B. Hay) and mouse anti-Hid (1:500; from A. Bergmann). Secondary antibodies were donkey Fab fragments from Jackson ImmunoResearch (West Grove, PA). BrdU incorporation was performed for 1 h⁶.

For *in situ* hybridization to detect *hpo* transcripts, *Drosophila* cDNA clone RE21564 (ResGen Invitrogen, Huntsville, AL) was used as a template to generate digoxigenin (DIG)-labelled RNA probes (Roche, Nutley, NJ). TdT-mediated dUTP nick end labelling (TUNEL) labelling was done on imaginal discs and pupal retinae by using an *in situ* cell death detection kit (Roche)¹⁹.

Protein production and co-immunoprecipitation. Full-length ³⁵S-labelled *Hpo* and *Sav* proteins were produced using the T7 *in vitro* transcription and translation system (Promega, Madison, WI). *Hpo* and *Sav* coding regions were amplified by PCR and subcloned into the T7plink vector, which contains the T7 promoter and the 5' untranslated leader from the β-globin gene fused to a Kozak consensus ATG, followed by multiple cloning sites. Myc-tagged proteins contained an N-terminal 9E10 Myc tag (MEQKLISEEDLNAGSEF). HA-tagged *Hpo* contained the HA tag (YPYDVPDYA) at position 483. *Sav* was tagged with the Myc epitope at its non-conserved N terminus. *Hpo* constructs contained the following amino acids: wild-type, 1–669; Δauto, 1–354/466–669; Δdimer, 1–597; ΔC-term, 1–474; kinase, 1–318; Δkinase, 323–669; and dimer, 590–669. *Sav* (cDNA clone RE52745; ResGen Invitrogen) constructs contained the following amino acids: wild-type, 1–607; ΔSD, 1–516; ΔWW, 1–414/491–609; N-term, 1–414; ΔN-term, 405–609; WW, 405–516; and SD, 491–609.

For co-immunoprecipitation, 7 μl of product from *in vitro* transcription and translation and 1 μg of monoclonal antibodies against Myc (Babco, Berkeley, CA) were added to 320 μl of immunoprecipitation buffer (15 mM HEPES (pH 7.9), 150 mM KCl, 1 mM EDTA, 1% Triton and 0.1% SDS) and incubated for 1 h at 4 °C. Next, 20 μl of protein-A-Sepharose (Amersham Pharmacia,

Piscataway, NJ) was added and the reaction was incubated on a shaker at 4 °C for 60 min. We collected the agarose beads by centrifugation at 1,500g for 2 min. Supernatant was removed and the beads were washed four times with 700 μl of cold immunoprecipitation buffer. Bound proteins were eluted and denatured in 40 μl of SDS sample buffer by incubation at 68 °C for 15 min. Proteins were separated by standard 10% and 15% SDS-PAGE gels. Gels were dried and exposed to BiomaxMR film (Kodak).

Yeast two-hybrid screen. We used the MATCHMAKER2 Two Hybrid System 3.0 (Clontech, Palo Alto, CA). Full-length *Drosophila sav* was cloned in frame with the GAL4 DNA-binding domain of the pGBKT7 vector. The construct was transformed into yeast strain AH109 and the resultant strain was tested for the expression of *Sav* and the absence of auto-activation. This strain was transformed with a *Drosophila* embryonic cDNA library in pACT2 (a gift from S. Elledge). We screened about 1.4 × 10⁶ colonies and sequenced 108 positive clones. Blast searches identified 20 genes that were represented by two or more independent clones. The *hpo* cDNAs isolated from the screen were transformed back into AH109 for reconstruction and confirmation of the interaction.

Note: Supplementary Information is available on the Nature Cell Biology website.

ACKNOWLEDGEMENTS

We thank K. Basler, H. J. Bellen, A. Bergmann, P. Bryant, K.-W. Choi, B. Dickson, B. Edgar, B. Hay, G. Mardon, M. Miura, A. Singh, the Bloomington *Drosophila* Stock Center, and the Developmental Studies Hybridoma Bank for fly stocks and antibodies; H. Jafar-Nejad for technical advice with the yeast-two-hybrid screen; G. Zhai for help with SNP detection by HPLC; P. R. Hiesinger for help with pupal stainings; J. Zhang for help with microinjections; K. Dunner for help with SEM, which along with DNA sequencing was done at M. D. Anderson core facilities, which is supported by a grant from the National Cancer Institute (CA16672); L. McCord for help with artwork; and H. J. Bellen, A. Bergmann, B. Frankfort, P. R. Hiesinger, R. Johnson, J. Kunz, S. Markus, K. Pappu, A. Singh and G. Zhai for discussion and comments on the manuscript. This publication was made possible by grants from the NIEHS (T32 ES07332) and the NICHD (HD07325) to R.U., and an NIH grant (GM067997), a Pharmacia Research Grant and a Basil O'Connor Award (FY01-497) to G.H.

COMPETING FINANCIAL INTERESTS

The authors declare that they have no competing financial interests.

Received 12 June 2003, accepted 26 August 2003.

Published online at <http://www.nature.com/naturecellbiology>

- Conlon, I. & Raff, M. Size control in animal development. *Cell* **96**, 235–244 (1999).
- Green, D. R. & Evan, G. I. A matter of life and death. *Cancer Cell* **1**, 19–30 (2002).
- Dan, I., Watanabe, N. M. & Kusumi, A. The Ste20 group kinases as regulators of MAP kinase cascades. *Trends Cell Biol.* **11**, 220–230 (2001).
- Justice, R. W., Zilian, O., Woods, D. F., Noll, M. & Bryant, P. J. The *Drosophila* tumor suppressor gene *warts* encodes a homolog of human myotonic dystrophy kinase and is required for the control of cell shape and proliferation. *Genes Dev.* **9**, 534–546 (1995).
- Xu, T., Wang, W., Zhang, S., Stewart, R. A. & Yu, W. Identifying tumor suppressors in genetic mosaics: the *Drosophila* *lats* gene encodes a putative protein kinase. *Development* **121**, 1053–1063 (1995).
- Kango-Singh, M. et al. Shar-pei mediates cell proliferation arrest during imaginal disc growth in *Drosophila*. *Development* **129**, 5719–5730 (2002).
- Tapon, N. et al. *salvador* promotes both cell cycle exit and apoptosis in *Drosophila* and is mutated in human cancer cell lines. *Cell* **110**, 468–478 (2002).
- Newsome, T. P., Asling, B. & Dickson, B. J. Analysis of *Drosophila* photoreceptor axon guidance in eye-specific mosaics. *Development* **127**, 851–860 (2000).
- Baker, N. E. Cell proliferation, survival, and death in the *Drosophila* eye. *Semin. Cell Dev. Biol.* **12**, 499–507 (2001).
- Neufeld, T. P., de la Cruz, A. F., Johnston, L. A. & Edgar, B. A. Coordination of growth and cell division in the *Drosophila* wing. *Cell* **93**, 1183–1193 (1998).
- Grether, M. E., Abrams, J. M., Agapite, J., White, K. & Steller, H. The head involution defective gene of *Drosophila melanogaster* functions in programmed cell death. *Genes Dev.* **9**, 1694–1708 (1995).
- White, K., Tahaoglu, E. & Steller, H. Cell killing by the *Drosophila* gene *reaper*. *Science* **271**, 805–807 (1996).
- Chen, P., Nordstrom, W., Gish, B. & Abrams, J. M. *grim*, a novel cell death gene in *Drosophila*. *Genes Dev.* **10**, 1773–1782 (1996).
- Christich, A. et al. The damage-responsive *Drosophila* gene *sickle* encodes a novel IAP binding protein similar to but distinct from *reaper*, *grim*, and *hid*. *Curr. Biol.* **12**, 137–140 (2002).
- Wing, J. P. et al. *Drosophila sickle* is a novel grim-reaper cell death activator. *Curr. Biol.* **12**, 131–135 (2002).
- Srinivasula, S. M. et al. *sickle*, a novel *Drosophila* death gene in the *reaper/hid/grim*

- region, encodes an IAP-inhibitory protein. *Curr. Biol.* **12**, 125–130 (2002).
17. Tenev, T., Zachariou, A., Wilson, R., Paul, A. & Meier, P. Jafra2 is an IAP antagonist that promotes cell death by liberating Dronc from DIAP1. *EMBO J.* **21**, 5118–5129 (2002).
 18. Yoo, S. J. *et al.* Hid, Rpr and Grim negatively regulate DIAP1 levels through distinct mechanisms. *Nature Cell Biol.* **4**, 416–424 (2002).
 19. Wang, S. L., Hawkins, C. J., Yoo, S. J., Muller, H. A. & Hay, B. A. The *Drosophila* caspase inhibitor DIAP1 is essential for cell survival and is negatively regulated by HID. *Cell* **98**, 453–463 (1999).
 20. Lisi, S., Mazzon, I. & White, K. Diverse domains of THREAD/DIAP1 are required to inhibit apoptosis induced by REAPER and HID in *Drosophila*. *Genetics* **154**, 669–678 (2000).
 21. Goyal, L., McCall, K., Agapite, J., Hartwig, E. & Steller, H. Induction of apoptosis by *Drosophila* reaper, hid and grim through inhibition of IAP function. *EMBO J.* **19**, 589–597 (2000).
 22. Berger, J. *et al.* Genetic mapping with SNP markers in *Drosophila*. *Nature Genet.* **29**, 475–481 (2001).
 23. Cheung, W. L. *et al.* Apoptotic phosphorylation of histone H2B is mediated by mammalian sterile twenty kinase. *Cell* **113**, 507–517 (2003).
 24. Graves, J. D. *et al.* Caspase-mediated activation and induction of apoptosis by the mammalian Ste20-like kinase Mst1. *EMBO J.* **17**, 2224–2234 (1998).
 25. Lee, K. K., Ohyama, T., Yajima, N., Tsubuki, S. & Yonehara, S. MST, a physiological caspase substrate, highly sensitizes apoptosis both upstream and downstream of caspase activation. *J. Biol. Chem.* **276**, 19276–19285 (2001).
 26. Creasy, C. L., Ambrose, D. M. & Chernoff, J. The Ste20-like protein kinase, Mst1, dimerizes and contains an inhibitory domain. *J. Biol. Chem.* **271**, 21049–21053 (1996).
 27. Kurada, P. & White, K. Ras promotes cell survival in *Drosophila* by downregulating hid expression. *Cell* **95**, 319–329 (1998).
 28. Bergmann, A., Agapite, J., McCall, K. & Steller, H. The *Drosophila* gene *hid* is a direct molecular target of Ras-dependent survival signaling. *Cell* **95**, 331–341 (1998).
 29. Yang, L. & Baker, N. E. Cell cycle withdrawal, progression, and cell survival regulation by EGFR and its effectors in the differentiating *Drosophila* eye. *Dev. Cell* **4**, 359–369 (2003).
 30. Deng, Y., Pang, A. & Wang, J. H. Regulation of mammalian STE20-like kinase 2 (MST2) by protein phosphorylation/dephosphorylation and proteolysis. *J. Biol. Chem.* **278**, 11760–11767 (2003).
 31. Johnston, L. A. & Gallant, P. Control of growth and organ size in *Drosophila*. *BioEssays* **24**, 54–64 (2002).
 32. Oldham, S. & Hafen, E. Insulin/IGF and target of rapamycin signaling: a TOR de force in growth control. *Trends Cell Biol.* **13**, 79–85 (2003).
 33. Turechalk, G. S., St John, M. A., Tao, W. & Xu, T. The role of LATS in cell cycle regulation and tumorigenesis. *Biochim. Biophys. Acta* **1424**, M9–M16 (1999).
 34. Brand, A. H. & Perrimon, N. Targeted gene expression as a means of altering cell fates and generating dominant phenotypes. *Development* **118**, 401–415 (1993).